P6.5 EVOLUTION OF A TORNADIC SUPERCELL AND ITS ENVIRONMENT SAMPLED BY THE PHASED ARRAY RADAR AND OKLAHOMA CITY MICRONET

Rick M. Hluchan *
University of Oklahoma/National Severe Storms Laboratory, Norman, Oklahoma

Pamela L. Heinselman, NOAA/ National Severe Storms Laboratory, Norman, Oklahoma

1. INTRODUCTION

Numerous studies have shown that a supercell can periodically undergo several life cycles during its lifetime; these storms are known as cyclic supercells (Beck et al. 2006; Wakimoto et al. 2003; French et al. 2008; Burgess et al. 1982). Some cyclic supercells can produce a number of tornadoes over their lifetime. This process is know as cyclic tornadogenesis and can occur many times within one supercell (Burgess et al. 1982; Dowell and Bluestein 2002). Every cyclic supercell, however, does not produce a tornado each time the supercell cycles (French et al. 2008).

The 10 February 2009 Oklahoma City cyclic, tornadic supercell is a unique event because it passed within close range of the National Weather Radar Testbed's Phased Array Radar (NWRT PAR). Previous studies have investigated the impact of the NWRT PAR's high–temporal resolution on the evolution of hail storms, microbursts, and non–tornadic supercells (Heinselman et al. 2008), but not a tornadic supercell. This supercell also moved over the northwest domain of a dense network of surface observing sensors known as the Oklahoma City Micronet. Having this high–temporal and spatial resolution radar and surface data affords an opportunity to investigate the detailed structure and evolution of the tornadic supercell.

Section 2 of this study describes this unique dataset further. The synoptic conditions preceding the event are discussed in section 3. Analysis of the low–level radar and surface data, found within section 4, provides observational insight regarding the process of cyclic tornadogenesis. Concluding remarks are found in section 5.

* *Corresponding author address:* Rick M. Hluchan, National Severe Storms Laboratory, 120 David L. Boren Blvd., Suite 4340, Norman, Oklahoma, 73072. E-mail: rick.hluchan@noaa.gov

The close range of the 10 February 2009 tornadic supercell to the PAR and high–resolution surface measurements from the Oklahoma Mesonet and Oklahoma City Micronet combine to form a unique dataset (Fig. 1). Each of these instruments is described in detail below.

Important operating characteristics of the NWRT PAR are given in Table 1; more details about the PAR are found in Zrnić et al. (2007). One significant advantage of the PAR is its antenna design. The antenna forms and steers the beam in azimuth and elevation electronically which allows the operator to focus on weather echo without moving the radar. The PAR is currently equipped with a single-faced phased array that scans sectors up to 90˚ in azimuth. Stationary scanning samples the atmosphere without beam smearing, while sector scanning provides high–temporal resolution data.

The Oklahoma City 10 February 2009 tornadic supercell passed within 50 km of the PAR, which scanned almost continuously throughout the evolution of the storm. During this event the radar was operated using two scanning strategies (Table 1). At the beginning of data collection (2023–2044 UTC), when the supercell was 37–41 km from the PAR, data were collected at 14 elevation angles between 0.51° and 15.50°. As the supercell moved beyond 41 km of the PAR (2044–2117 UTC) data were collected between the angles of 0.51° and 38.80°. Both scanning strategies completed a full volume scan in approximately 70 s; however the lowest tilt was revisited halfway through the scan to improve temporal resolution at that level. Lowest elevation angle (0.51°) beam heights relative to the circulation were 0.8 km AGL at the beginning of data collection and 1 km AGL at the end of the period of interest.

PAR Operating Characteristics	
Wavelength	9.38 cm
Transmitted peak power	750 kW
Range resolution	240 m
Half–power beamwidth	1.50°–2.10°
Azimuthal sample interval	1.0°
Nyquist velocity	23.8 m s^{-1}
Elevation angles	0.51°–15.50°; 0.51°–38.80° 14 elevations
Data interval	32–70 sec
Range to tornado	38–55 km
0.51° beam height	0.8–1 km

Table 1. PAR radar and scanning strategy characteristics for 10 February 2009.

As the supercell moved across Oklahoma County the hook echo passed over the northwest domain of the Oklahoma City Micronet (OKCNET; Basara et al. 2009). The OKCNET was developed following the Joint Urban 2003 (JU2003) field experiment conducted in the central business district of Oklahoma City (Allwine et al. 2004). After years of designing and testing, JU2003 transformed into a much larger project designed to improve atmospheric monitoring across the Oklahoma City metropolitan area. The OKCNET was commissioned in 2008 into an operational network of 40 atmospheric monitoring sensors mounted on traffic signals (approximately 9 m AGL) in Oklahoma City. Three of the 40 sensors are recently installed Oklahoma Mesonet stations. The Oklahoma City Micronet observes atmospheric conditions at a fine spatial resolution with an average station spacing of approximately 3 km. Atmospheric data are measured and transmitted every minute to the Oklahoma Climatology Survey (OCS) where the data is quality controlled and made available to the public. More information on the OKCNET can be obtained from Basara et al. (2009).

The Oklahoma Mesonet also measured atmospheric conditions before and during supercell development (Brock et al. 1995; McPherson et al. 2007). Like the OKCNET, the Oklahoma Mesonet is an automated atmospheric monitoring network with instruments at 9 m, but also at 1.5 m. Only 1.5 m Mesonet data were used in this study as it better sampled near–surface atmospheric conditions. The Oklahoma Mesonet includes 110 stations; at least one station is located in each county. Quality–assured data is measured, transmitted and available every 5 min to the public through the OCS (Brock et al. 1995, McPherson et al. 2007).

The local prestorm environment was also measured by an 1800 UTC sounding launched at Norman, Oklahoma within an hour and approximately 80 km from the first weather echo observed on radar.

3. SYNOPTIC SETTING

During the early afternoon hours, a strong surface low pressure system was positioned over Minnesota with a returning warm front located over southern Oklahoma (Fig. 2). A north–south oriented dryline extended across western Oklahoma where a sharp moisture gradient existed. The 1800 UTC Norman sounding showed moisture had significantly increased since 1200 UTC throughout the mid– and low–levels of the atmosphere (Fig. 3). Sounding analysis for 1800 UTC showed convective available potential energy (CAPE) values near 500 J kg^{-1} within the area of strong insolation where storms formed (Fig. 2). A developing jet streak at 300 hPa supported an area of upper–level divergence over much of the Southern Plains (e.g., Uccellini and Johnson 1979). A series of shortwave troughs at 700 mb aided lift over central Oklahoma. An intense upper low and associated long wave trough was approaching from the southwest US, acting to increase both speed and directional wind shear for supercell development. Shear values from 0–1 km were near 15 m s^{-1}. The advancing trough likely induced cyclogenesis near and northwest of the aforementioned baroclinic zone. Winds at the surface began to increase and back to the southeast with time in response to a developing low over southeastern Colorado (Fig. 2). This

change in wind direction helped to increase moisture and direction shear.

4. DATA ANALYSIS

Previous studies of low- and midlevel, storm–scale circulations usually classify them based on predefined criteria such as the diameter, vertical vorticity, and/or the radial velocity (e.g., Burgess et al. 2002; French et al. 2008; Beck et al. 2006; Wakimoto et al. 2003). Also taken into account is the height (AGL) at which the circulation is located. In this study, the circulation of interest changes the diameter and radial velocity frequently. To capture its evolution, criteria for defining a circulation: a diameter of 1–10 km, a minimum velocity difference between inbound and outbound velocities of 15 m s^{-1} that exists for at least two consecutive volume scans or 2 min. These criteria are similar to French et al. (2008).

This study examines two cycles of a cyclic, tornadic supercell in which each time period analyzed focuses on one complete cycle, including the organization of the low–level circulation associated with the hook echo, the intensification of the circulation and subsequent tornado, and the dissipation of the circulation and hook echo.

During the supercells' lifetime, it moved from 239° with a speed of 19.7 m s^{-1}. For brevity, the evolution of the supercell in reflectivity and storm–relative velocity are shown approximately every 3–6 min, even though complete volume scans were done at ~70 s intervals (Figs. 4 and 6). At the 0.50° elevation angle, the supercell was sampled at heights from approximately 0.8–1.0 km, depending on the echoes' range from the radar. Analysis of the full storm is in progress though the focus here is on the 0.5° elevation.

4.1 Evolution of hook and low-level circulation: 2022:58–2037:03 UTC

The first full scan sampling the entire supercell was at 2022:58 UTC when the hook echo was located about 38 km west-northwest of the radar site (Fig. 4a). The storm was well organized with an intense rain and hail core located north of the reflectivity appendage developing on the southwest flank of the storm. Associated with the hook was a strengthening rear–flank gust front (RFGF). An area of strong inbound storm–relative velocities (24 m s^{-1}) existed ahead of the advancing RFGF, producing a well–defined inflow notch (Fig. 4a).

By 2028:49 UTC the hook grew wider in diameter with a "knob" like structure forming on its southeast side (Fig. 4b). This feature is thought to be created by debris being lofted by a tornado (Burgess et al. 2002); however one was not observed at this time. The circulation associated with the hook intensified with the maximum velocity difference increasing from 29 m s^{-1} to 34 m s^{-1} (2022:58–2028:49 UTC). Southeast of the supercell is a new elongated area of precipitation that can be seen forming southeast of the supercell (Fig. 4b).

At 2034:41 UTC, the new area of precipitation merged with the supercell creating a muddled appearance to the hook echo (Fig. 4c). Following the merger, approximately 1 min later, the circulation contracted and strengthened. The storm–relative velocity difference peaked near ~40 m s^{-1} for two volume scans (2034:41–2035:51) likely causing the circulation to be sampled less by an operational 4–6 min scanning strategy. The corresponding increase in the velocity field was associated with the supercells' first tornado. The EF1 tornado tracked 1.2 km through a northwest Oklahoma City shopping center producing minor damage and only lasted ~1 min (Fig. 1).

A few minutes later, at 2037:03 UTC, the hook was still filled with precipitation and the very intense circulation associated with the first tornado had almost completely dissipated (Fig. 4d). It is also during this time (2037–2039 UTC) that the supercells' hook echo began to move over the Oklahoma City Micronet. The Micronet captured a convergent cyclonic circulation at the surface along a bulge in the RFGF created by an extensive cold pool (Fig. 5). A new circulation began to develop just east of the previous circulation, near the bulge in the northeast segment of the RFGF (Figs. 4d and 5).

4.2 Evolution of hook and low–level circulation: 2042:55–2105:20 UTC

The evolution of the second cycle of the tornadic supercell was very similar to the first cycle. By 2042:55 UTC, the hook echo was located 42 km north–northwest of the PAR (Fig. 6a). The hook had regenerated and become more well–defined, as it was 20 min earlier, before an area of precipitation merged with it (Fig. 4a). On the reflectivity scan at 2042:55 UTC, a small area of precipitation is located just east of the hook echo. Between 2037:03 and 2042:55 UTC, the circulation contracted and intensified with a maximum velocity difference of 30 m s^{-1}.

At 2046:34 UTC, the newly developed area of precipitation had moved northwest within the inflow of the supercell and circulation strength was

similar to that at 2042:55 UTC (Fig. 6b). The hook echo and the once separated area of precipitation merged, again causing the hook echo to appear less–defined by 2051:16 UTC (Fig. 6c). The circulations' intensity increased to a maximum storm–relative velocity difference of 34 m s^{-1} (Fig. 6c). Shortly after the area of precipitation merged with the hook echo (2053 UTC), the supercell produced its second tornado. This tornado was on the ground for approximately 12 min with a 10.5 km long path (Fig. 1). The damage associated with this tornado was rated EF2 as it tore through several homes. Storm–relative velocity scans showed this intense circulation for several minutes with a peak velocity difference of 42 m s^{-1} at 2057:07 UTC (Fig. 6d). Also at this time, the hook echo exhibited a knob feature at its tip as it did in the first cycle. This time however, the knob is likely related to debris being lifted into the atmosphere by the tornado.

The storm–relative velocity image shows the RFGF becoming less–defined and its speed slowed from 15.3 m s^{-1} to 9.3 m s^{-1} (Figs. 6c–d). With the supercell ~47 km from the radar, the 0.50° elevation beam is overshooting (0.9 km AGL) the majority of the gust front causing it to appear less clear. A possible reason for the gust front reducing its speed is that the inflow from another supercell to the southwest of the parent storm is opposing the forward progression of the cold pool. The circulation associated with the tornado fell below the 15 m s^{-1} velocity difference criteria soon after the tornado lifted at 2105:20 UTC (not shown). The circulations associated with both cycles of the supercell were shallow in nature, never extending above 2.5 km AGL.

5. SUMMARY

The 10 February 2009 Oklahoma City cyclic, tornadic supercell represents a unique case in which high–temporal and spatial resolution data was collected by the PAR and the Oklahoma City Micronet. The combination of increased temporal and spatial resolution revealed rapidly evolving circulations; perhaps too quick to be detected with a more conventional scanning strategy of 4–6 min.

The storm exhibited cyclic tornadogenesis, allowing the comparison of cyclic structure between this storm and other studies of cyclic supercells. The evolution of the hook echo mostly followed the conceptual model of Beck et al. (2006) as it regenerated during the second cycle of the supercell. Both cycles examined here featured a broad, low–level circulation periodically intensifying to produce a tornado. At the end of the first cycle, after the first tornado had lifted, a new circulation formed along a bulge in the rear flank gust front. This new circulation went on to become the primary circulation during the second cycle of the supercell.

During both cycles of the supercell, an area of precipitation formed southeast of the hook echo and moved toward the north within the storm's inflow. Shortly after (approximately 1 min) the area of precipitation merges with the hook echo in both cycles, the circulation intensifies and a tornado is produced. The surging cold pool and associated gust front may have ultimately undercut the low–level circulation causing the tornado to dissipate. After the time period of synthesis, the supercell may have once again cycled; however, it is difficult to track the progress of the gust front after the second cycle of the supercell as it moves farther away from the radar.

Future analyses will asses the midlevels of the supercell as well as examine a comparison of the cyclic nature of this supercell and other studies containing high–temporal and spatial resolution data.

Acknowledgements. The authors would like to thank Dave Andra and Patrick Burke of the Norman WFO for providing insight on the synoptic conditions. We further recognize: Jeff Basara of the Oklahoma Climate Survey for helping provide the Oklahoma City Micronet data and Kevin Manross (CIMMS/NSSL) for his technical contributions to display the data.

REFERENCES

Allwine, K. J., M. J. Leach, L. W. Stockham, J. S. Shinn, R. P. Hosker, J. F. Bowers, and J. C. Pace, 2004: Overview of Joint Urban 2003–An atmospheric dispersion study in Oklahoma City. *Symp. On Planning, Nowcasting, and Forecasting in the Urban Zone*, Seattle, WA, Amer. Meteor. Soc.

Basara, J. B., B. G. Illston, C. A. Fiebrich, R. A. McPherson, J. P. Bostic, P. Browder, D. B. Demko, C. Morgan, and K. Kesler, 2009: An overview of the Oklahoma City Micronet. Preprints, *8th Symposium on the Urban Environment*, Phoenix, AZ, Amer. Meteor. Soc., J1.1.

Beck, J. R., J. L. Schroeder, J. M. Wurman, 2006: High-resolution dual-doppler analyses of the 29 May 2001 Kress, Texas, cyclic supercell. *Mon. Wea. Rev.*, **134**, 3125–3148.

Brock, F. V., K. C. Crawford, R. L. Elliott, G. W. Cuperus, S. J. Stadler, H. L. Johnson, and M.

D. Eilts, 1995: The Oklahoma Mesonet: A technical overview. *J. Atmos. Oceanic Technol.,* **12**, 5–19.

Burgess, D. W., M. A. Magsig, J. Wurman, D. C. Dowell, and Y. Richardson, 2002: Radar observations of the 3 May 1999 Oklahoma City tornado. *Wea. Forecasting*, **17**, 456–471.

——, V. T. Wood, and R. A. Brown, 1982: Mesocyclone evolution statistics. Preprints, *12th Conf. on Severe Local Storms,* San Antonio, TX, Amer. Meteor. Soc., 422–424.

Dowell, D. C., and H. B. Bluestein, 2002: The 8 June 1995 McLean, Texas, storm. Part I: Observation of cyclic tornadogenesis. *Mon. Wea. Rev.,* **130**, 2626–2648.

French, M. M., H. B. Bluestein, D. C. Dowell, L. J. Wicker, M. R. Kramar, and A. L. Pazmany, 2008: High-resolution, mobile Doppler radar observations of cyclic mesocyclogenesis in a supercell. *Mon. Wea. Rev.*, **136**, 4997–5016.

Heinselman, P. L., D. L. Preiegnitz, K. L. Manross, T. M. Smith, and R. W. Adams, 2008: Rapid sampling of severe storms by the National Weather Radar Testbed Phased Array Radar. *Wea. Forecasting,* **23**, 808–824.

McPherson, R. A., C. Fiebrich, K. C. Crawford, R. L. Elliott, J. R. Kilby, D. L. Grimsley, J. E. Martinez, J. B. Basara, B. G. Illston, D. A. Morris, K.A. Kloesel, S. J. Stadler, A. D. Melvin, A. J. Sutherland, and H. Shrivastava, 2007: Statewide monitoring of the mesoscale environment: A technical update on the Oklahoma Mesonet. *J. of Atmos. Oceanic Technol.,* **24**, 301–321.

Schneider, D., and S. Sharp, 2007: Radar signatures of tropical cyclone tornadoes in central North Carolina. *Wea. Forecasting*, **22**, 278–286.

Uccellini, L. W., and D. R. Johnson, 1979: The coupling of upper and lower tropospheric jet streaks and implications for the development of severe convective storms. *Mon. Wea. Rev.*, **107**, 682–703.

Wakimoto, R. M., H. V. Murphey, D. C. Dowell, H. B. Bluestein, 2003: The Kellerville tornado during VORTEX: Damage survey and Doppler radar analyses. *Mon. Wea. Rev.*, **131**, 2197–2221.

Zrnic, D. S., J. F. Kimpel, D. E. Forsyth, A. Shapiro, G. Crain, R. Ferek, J. Heimmer, W. Benner, T. J. McNellis, and R. J. Vogt, 2007: Agile–beam phased array radar for weather observations. *Bull. Amer. Meteor. Soc*., **88**. 1753–1766.

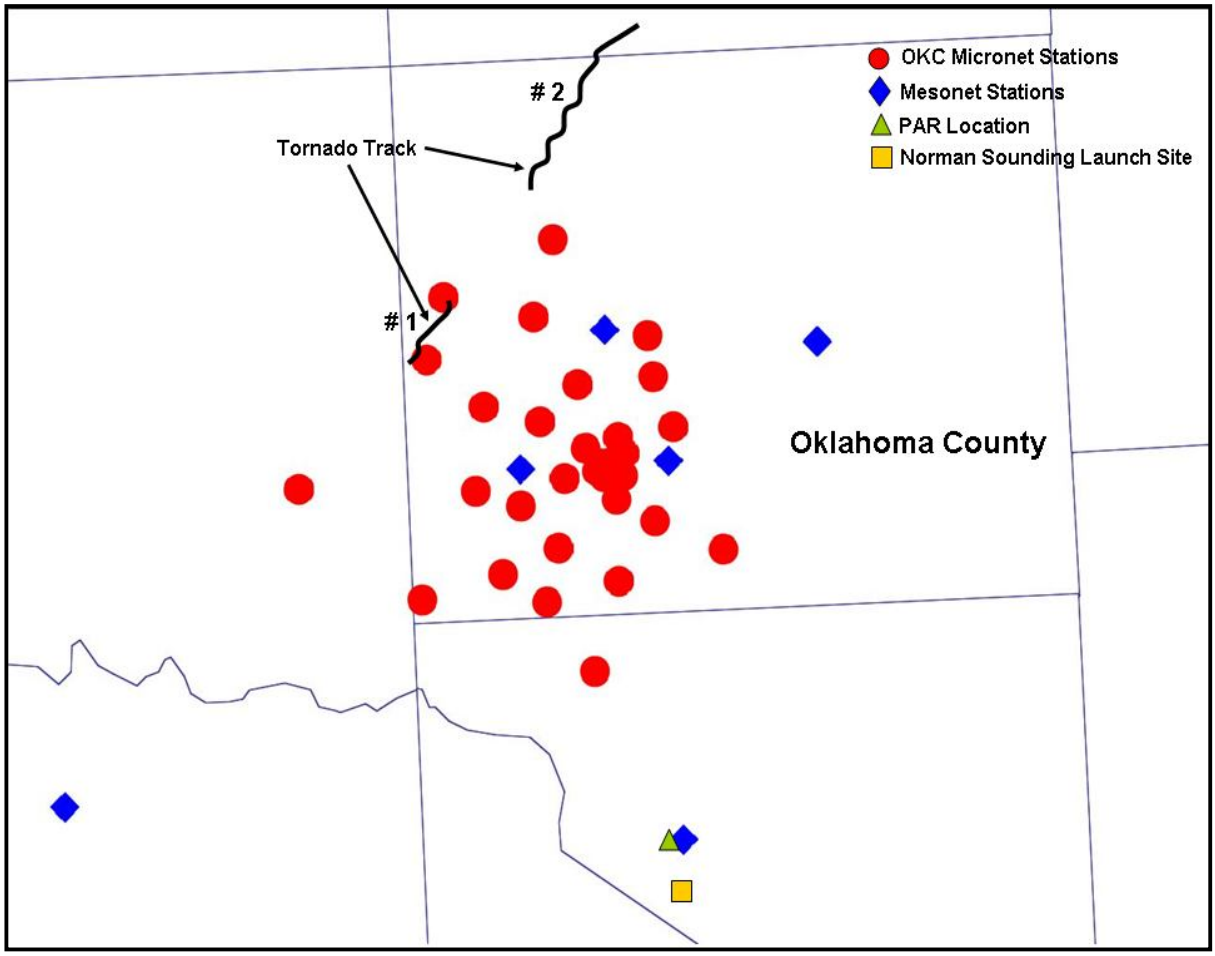

Fig. 1. Tornado tracks and locations of Oklahoma City Micronet and Mesonet stations, PAR, and the Norman sounding launch site.

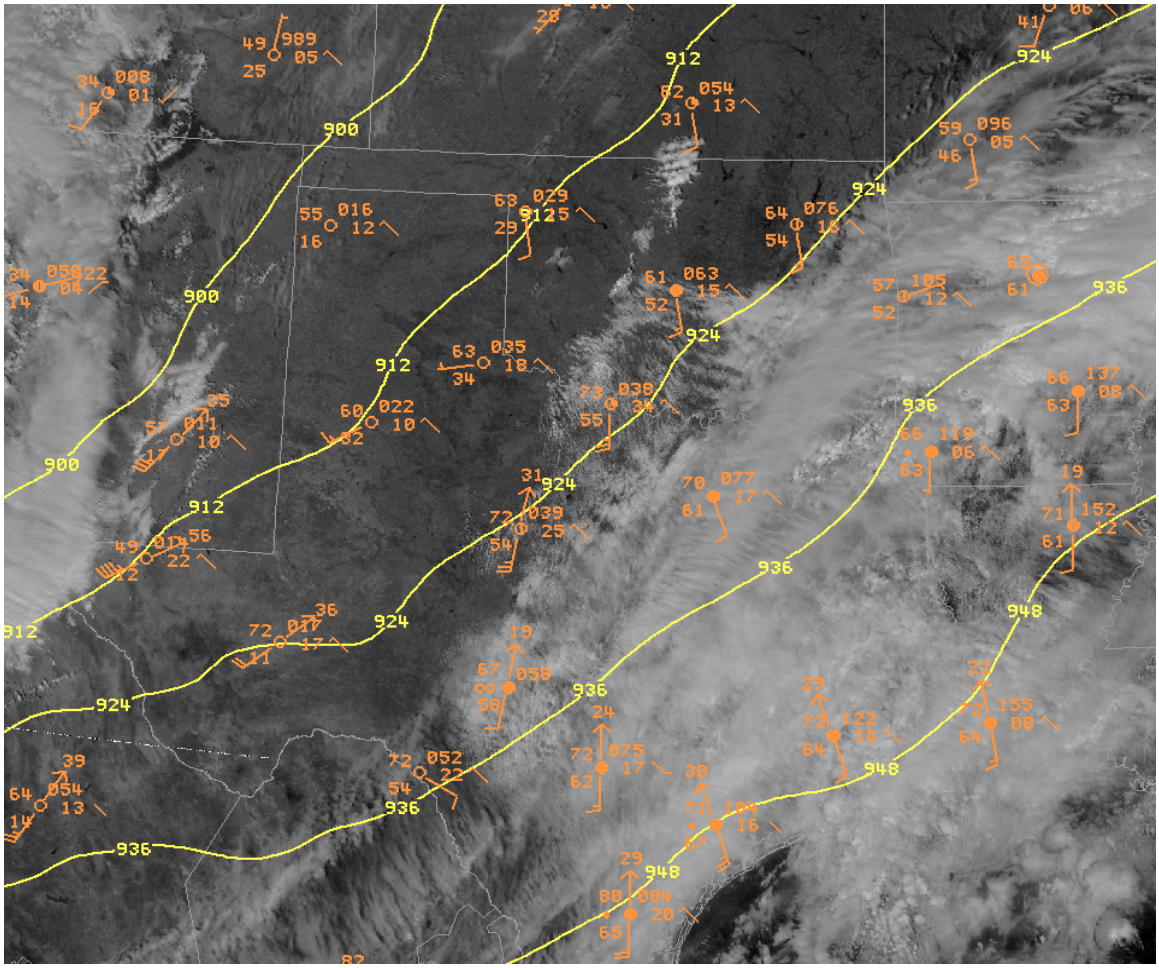

Fig. 2. Composite of surface measurements, 300mb upper air analysis, and *GOES-8* visible image at 1800 10 February 2009. For each station in orange, the temperature (upper left) and dewpoint (lower left) are in °F, and the altimeter setting (right) is in tenths of mb with leading "10" removed. Full (half) wind barbs represent 5 (2.5) m s^{-1}. Pressure tendency (middle right) is pressure change in past 3 hours to nearest tenth of mb. Yellow lines indicate RUC 300mb height analysis in (dam). Cloud features and surface observations provide evidence of the location of the moisture gradient in western OK.

(a)

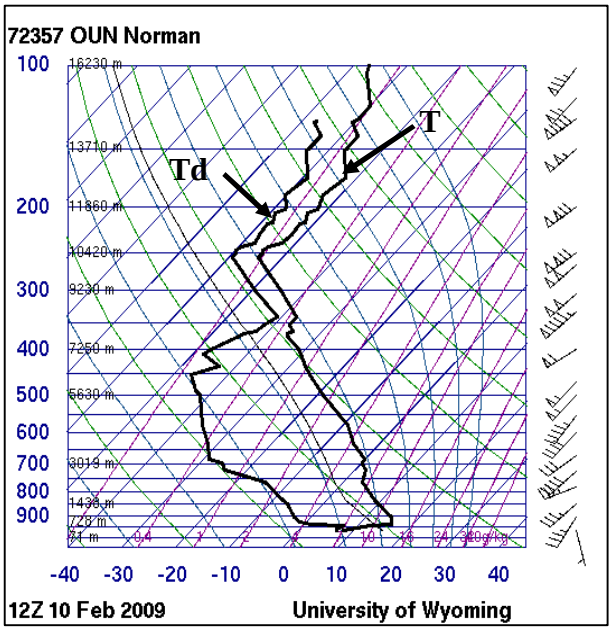

(b)

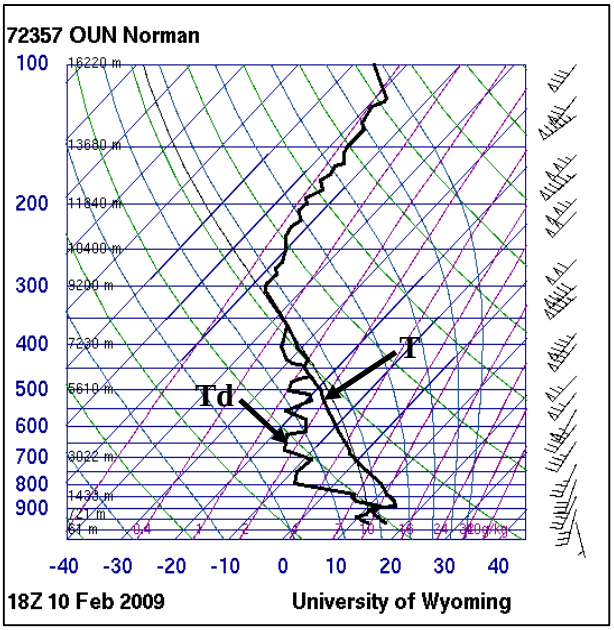

Fig. 3. Environmental conditions near the Oklahoma City supercell. Norman sounding at (a) 1200 UTC and (b) 1800 UTC 10 February 2009. Temperature (T) and dewpoint (Td) are in °C, pressure (left) in mb, and height in m AGL. Wind barbs and flags represent 10 kt (~5 m s^{-1}) and 50 kt (~25 m s^{-1}), respectively.

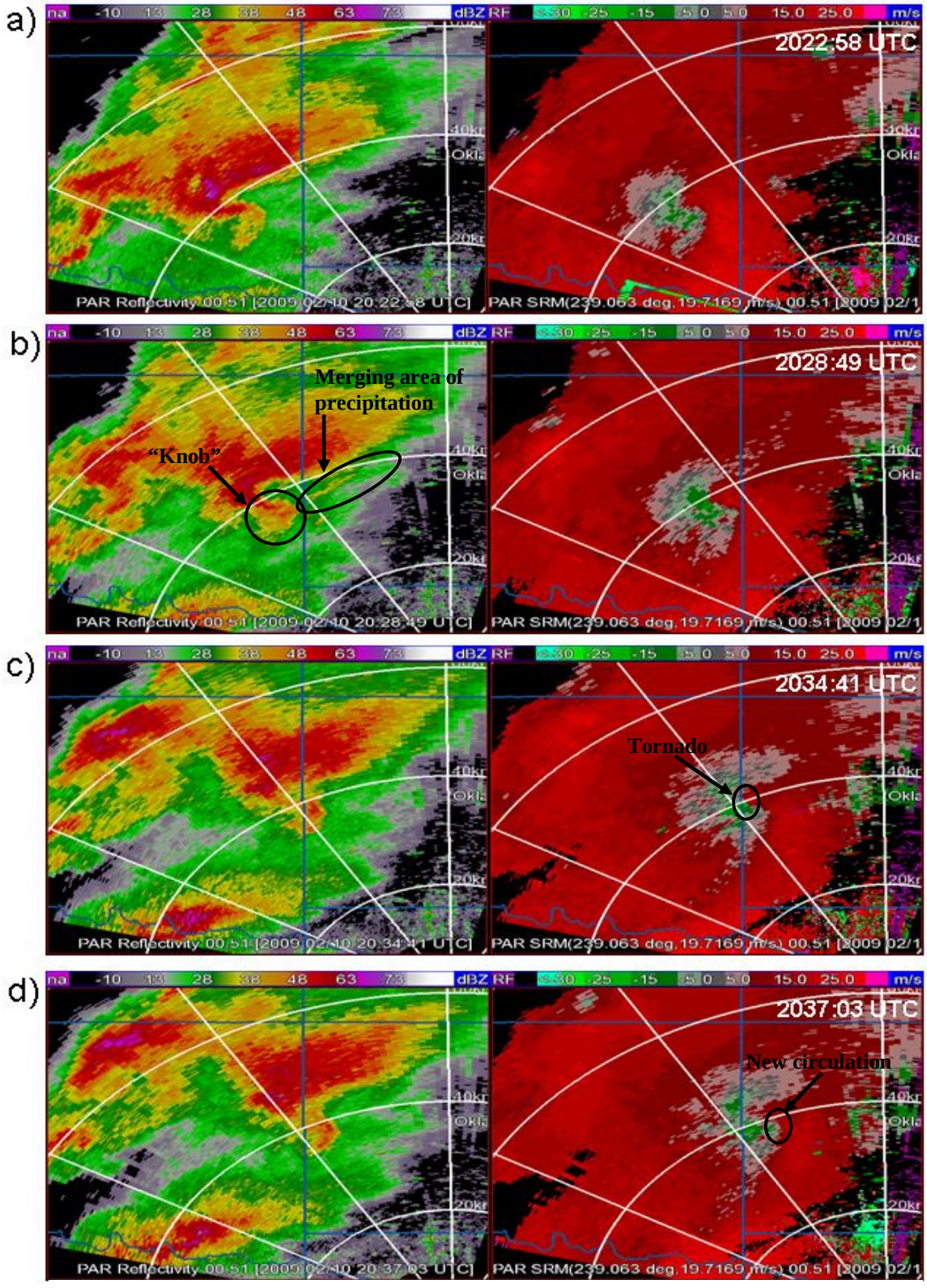

Fig. 4. Reflectivity factor (dBZ) and storm–relative velocity (m s^{-1}) (scales shown on top of each image) at 0.51° elevation angle from the NWRT PAR on 10 February 2009. Range rings (white) are every 20 km. Blue lines are county borders: (a) 2022:58, (b) 2028:49, (c) 2034:41, and (d) 2037:03 UTC.

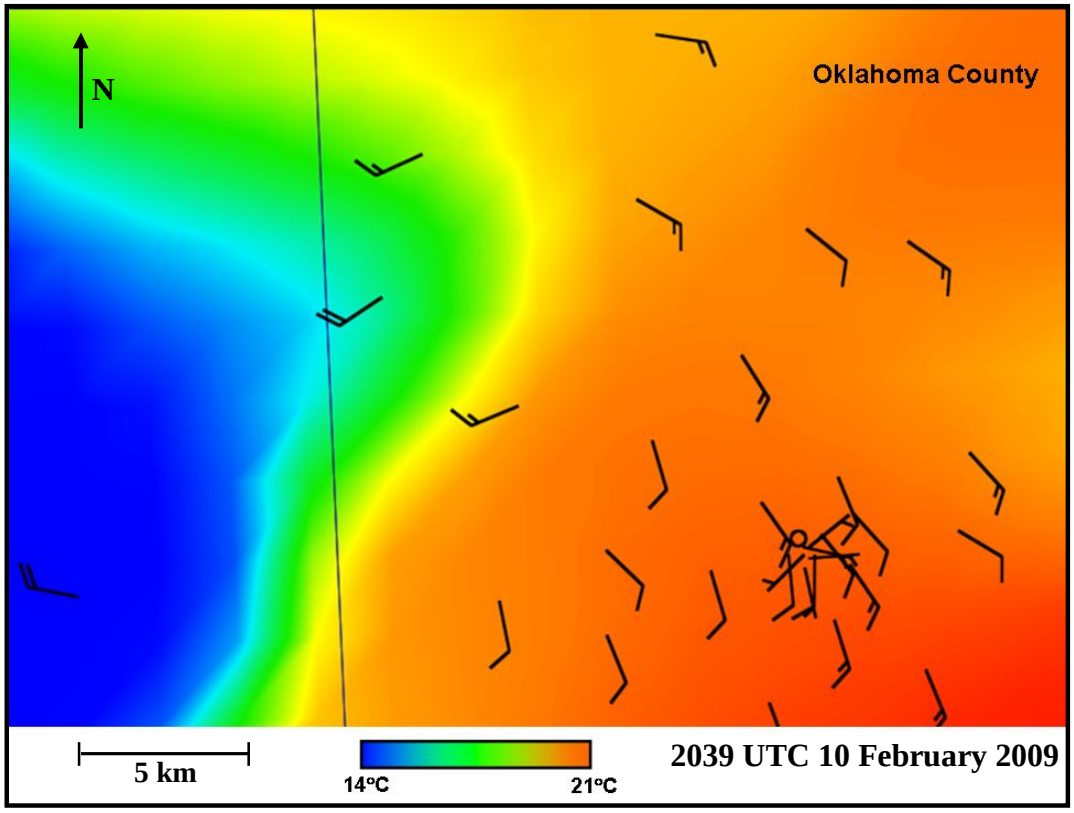

Fig. 5. Composite of Oklahoma City Micronet and Oklahoma Mesonet surface analysis temperature in °C and wind vectors (full barb = 5) m s^{-1} at 10 m AGL. Sharp temperature gradient in western Oklahoma Co. shows gust front with cyclonic circulation at bulge in front.

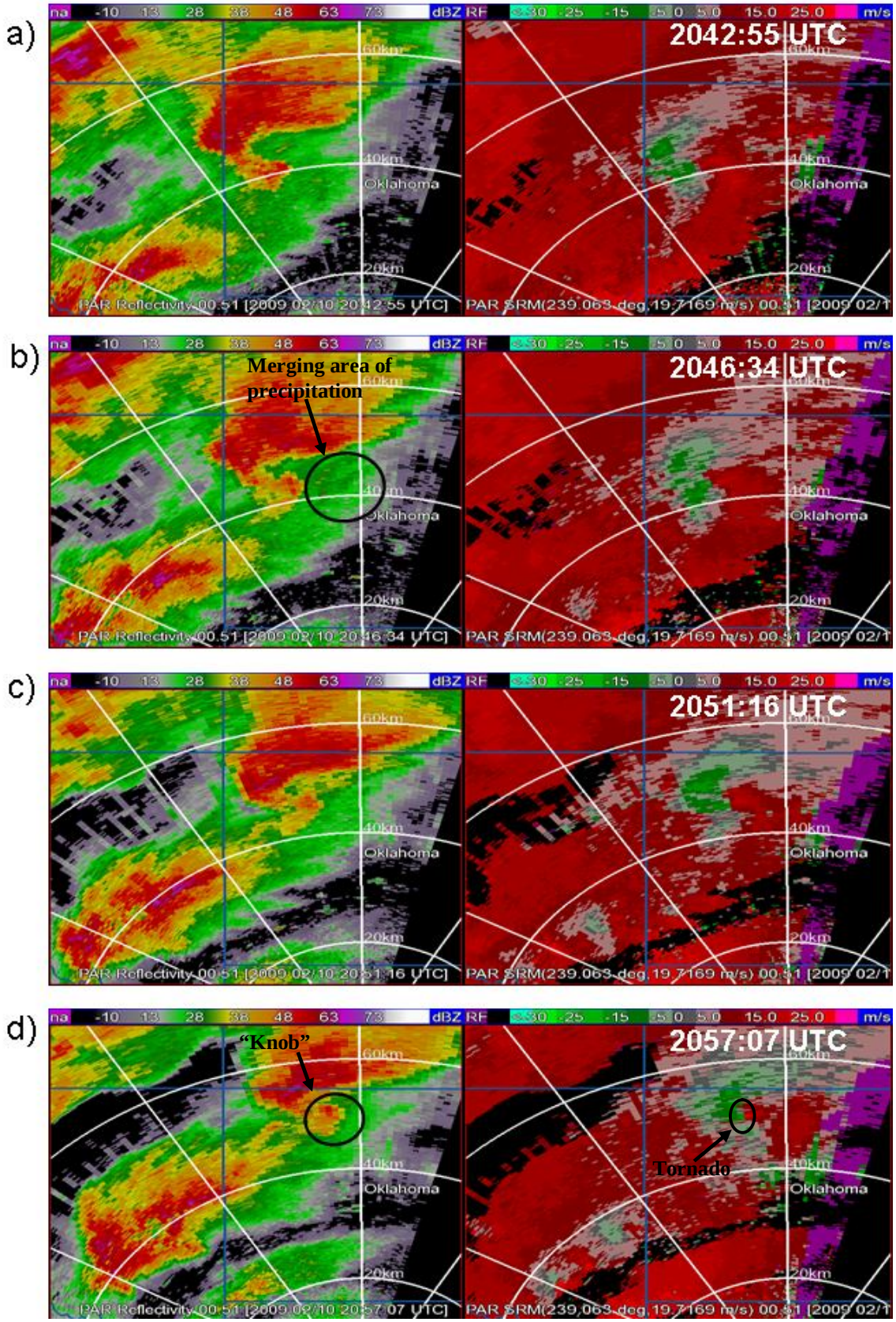

Fig. 6. As in Fig. 4, but: (a) 2042:55, (b) 2046:34, (c) 2051:16, and (d) 2057:07 UTC.